Development of RApid REsponse (RARE) System for Motorway Bridges: Overview and Pilot Application to Attiki Odos Motorway

Ioannis Anastasopoulos, *Professor, ETH Zürich, Zurich, Switzerland; email: ioannis.anastasopoulos@igt.baug.ethz.ch*

Panagiotis Ch. Anastasopoulos, *Associate Professor, Department of Civil, Structural and Environmental Engineering, SUNY at Buffalo; Inst. for Sustainable Transportation and Logistics; and Engineering Statistics and Econometrics Application Research Laboratory, Buffalo, NY, USA; email: panastas@buffalo.edu*

Lampros Sakellariadis, *PhD Candidate, ETH Zürich, Zurich, Switzerland; email: lampros.sakellariadis@igt.baug.ethz.ch*

Athanasios Agalianos, *PhD Candidate, ETH Zürich, Zurich, Switzerland; email: athanasios.agalianos@igt.baug.ethz.ch*

Rallis Kourkoulis, *Technical Director, GRID Engineers, Athens, Greece; email: info@grid-engineers.com*

Fani Gelagoti, *Assistant Director, GRID Engineers, Athens, Greece; email: info@grid-engineers.com*

George Gazetas, *Professor, National Technical University of Athens, Athens, Greece; email: gazetas@central.ntua.gr*

ABSTRACT: *Safety of motorway users in case of a strong seismic event is directly related to the performance of infrastructure elements, especially motorway bridges. Preventive closure until post–seismic inspection may seem as the safest option, but will unavoidably lead to severe deterioration of serviceability, and will also obstruct the operations of rescue teams. On the other hand, allowing traffic on earthquake–damaged bridges without inspection may jeopardize the safety of users and rescue teams. Seismic retrofit is the obvious solution, but the associated costs can be quite substantial. An alternative strategy is to mitigate the indirect consequences of an earthquake, through timely development and implementation of a RApid REsponse (RARE) system. The scope of such a RARE system is to ensure the safety of motorway users, minimizing motorway network closure, and optimizing post-seismic recovery at the same time. The development of such a RARE system requires an effective means to estimate seismic damage in real time. This paper presents an overview of the RARE system and some first steps that were made regarding its pilot application in the Attiki Odos Motorway in Athens, Greece.*

KEYWORDS: seismic vulnerability, real-time damage assessment, nonlinear analysis, regression models

SITE LOCATION: Geo-Database

INTRODUCTION

Under normal conditions, the safety of motorway users is a function of the quality of the roadway network (geometry, traffic characteristics, pavement condition) and the behavior of drivers (Russo et al., 2014; Sarwar & Anastasopoulos, 2016a, 2016b; Fountas et al., 2017; Fountas & Anastasopoulos, 2017; Sarwar et al., 2017). However, in the case of a strong earthquake, the safety of the users is directly related to the seismic performance of motorway infrastructure.

Even if a motorway bridge is still standing after the main shock, it may be severely damaged and therefore prone to collapse when subjected to aftershocks (Franchin & Pinto, 2009). Preventive closure until post–seismic inspection may seem as the safest option, but will unavoidably lead to a severe deterioration of serviceability, and will also obstruct the operations of rescue teams. On the other hand, allowing traffic on earthquake–damaged bridges without inspection may jeopardize the safety of users and rescue teams. As a result, after a strong earthquake the motorway administrator will face the question

whether or not to interrupt the operation of the network. Seismic retrofit is the obvious solution, but the associated costs can be quite substantial. An alternative strategy is to focus on the mitigation of the indirect consequences of a seismic event, through timely development and implementation of a RApid REsponse (RARE) system. The scope of such a RARE system is to ensure the safety of motorway users, minimizing motorway network closure, and optimizing post-seismic recovery at the same time.

In the last decade or so, a number of emergency response systems have been developed worldwide (e.g., Erdik et al., 2011). Apart from major global earthquake management systems, such as the Global Disaster Alert and Coordination System (GDACS, www.gdacs.org; De Groeve et al., 2006) and WAPMERR (www.wapmerr.org), several local systems have been developed to estimate casualties and infrastructure damage in near–real time for large cities such as Tokyo, Istanbul, and Naples (Erdik et al., 2003). In most cases, strong motion recordings are used to estimate the damage using an inventory of exposed elements and related vulnerability relations. In the case of transportation networks, there have been some first attempts to apply seismic risk assessment to motorway systems, as for example in the Friuli-Venezia Giulia region of NE Italy (Codermatz et al., 2003).

The framework of a RApid REsponse (RARE) system for metropolitan motorways has been introduced in Anastasopoulos et al. (2015a). Its development and implementation requires an effective means to estimate the seismic damage of motorway components (such as bridges, tunnels, retaining walls, cut slopes, and embankments) in real time, immediately after a seismic event. Real-time damage estimation is necessary to allow rational decisions with respect to the need for emergency inspection, and if necessary, the allocation of inspection teams. The goal is to minimize disruption and optimize post-seismic serviceability and recovery of the motorway network. This paper presents an overview of the RARE system and some first steps that were made regarding its pilot application in the Attiki Odos Motorway in Athens, Greece.

OVERVIEW OF THE RARE FRAMEWORK

A RARE system for motorway bridges is presented herein as part of a European research project, using the Attiki Odos Motorway (Athens, Greece) as a case study. As shown in Fig. 1, during a seismic event the real-time system will record seismic accelerations at various locations along the motorway. In this way, the seismic motion will be available in real time, right after the occurrence of the earthquake. For each bridge, the nearest record(s) will be used to assess the seismic damage employing the proposed real-time damage assessment system. The direct knowledge of the seismic excitation along the motorway is a major difference to traditional risk assessment, in which case the seismic excitation cannot possibly be predicted, and hence probabilistic approaches are much more appropriate.
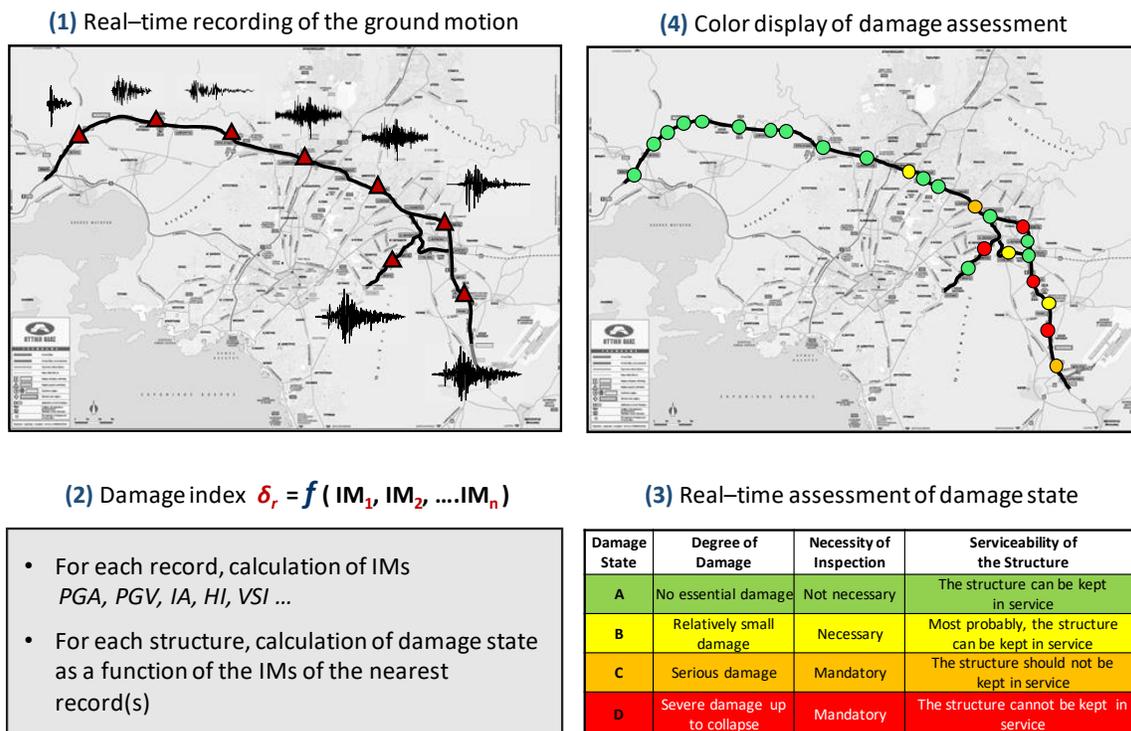
(1) Real–time recording of the ground motion

(4) Color display of damage assessment

(2) Damage index $\delta_r = f$ (IM_1, IM_2, ...IM_n)

- For each record, calculation of IMs
  PGA, PGV, IA, HI, VSI …

- For each structure, calculation of damage state as a function of the IMs of the nearest record(s)

(3) Real–time assessment of damage state

Damage State	Degree of Damage	Necessity of Inspection	Serviceability of the Structure
A	No essential damage	Not necessary	The structure can be kept in service
B	Relatively small damage	Necessary	Most probably, the structure can be kept in service
C	Serious damage	Mandatory	The structure should not be kept in service
D	Severe damage up to collapse	Mandatory	The structure cannot be kept in service

Figure 1. Schematic illustration of the application of the RARE system during a seismic event.

Four steps are required for the implementation (before the earthquake) of the RARE system. First of all (Step 1), a comprehensive GIS database of motorway infrastructure needs to be developed, including all the necessary information to describe the motorway and its key components. Subsequently (Step 2), a network of accelerograph stations needs to be installed, which will record the seismic motions at characteristic locations along the motorway. Then (Step 3), for each class of bridges, nonlinear dynamic time history analysis is performed using multiple seismic records as seismic excitation. Finally (Step 4), for all seismic excitations the corresponding intensity measures (IMs) are computed, and based on the results of the finite element (FE) analyses, a dataset correlating a damage index (DI) with various IMs is developed. The latter is used to develop a multivariate econometric model, expressing the seismic damage as a function of the most statistically significant IMs.

Real–Time Damage Assessment Methodology

The rapid damage assessment method outlined in Anastasopoulos et al. (2015a) combines finite element (FE) simulations with advanced econometric modeling. For each bridge type, the method requires: (a) nonlinear dynamic time history analyses using an adequately large number of real records as seismic excitation; (b) development of a dataset of the seismic damage, expressed by appropriate damage indices (DIs), as a function of the seismic excitation, which can be expressed by a variety of intensity measures (IMs); and (c) development of nonlinear regression models, expressing the seismic damage (using one or more DIs) as a function of statistically significant IMs. For the nonlinear dynamic time history analyses, an ensemble of 30 real records from earthquakes of various intensities and kinematic characteristics were carefully chosen and used as seismic excitation (Fig. 2). In a similar manner to the IDA methodology (Vamvatsikos & Cornell, 2002), each record is scaled to PGA ranging from 0.1 g to 1 g, yielding a dataset of 300 seismic excitations.
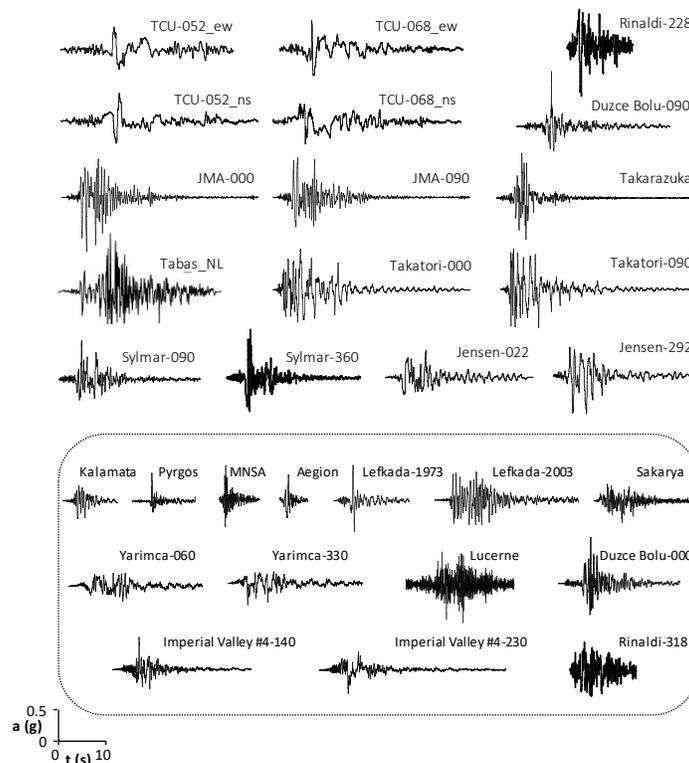

Figure 2. Real records used as seismic excitations for the nonlinear dynamic time history analyses.

In contrast to previous research on the subject, which aimed at identifying efficient IMs (e.g., Housner, 1952; Arias, 1970), the proposed RARE framework develops nonlinear regression models, combining an optimum number of statistically significant IMs. Previous studies have shown that a single IM is not always adequate to capture all of the characteristics of a seismic motion (e.g., Garini & Gazetas, 2013). In Anastasopoulos et al. (2015a), this was demonstrated using an idealized (single) bridge pier, which was considered as a SDOF system. One such example is shown in Fig. 3a, referring to the correlation of one of the most efficient IMs, the Velocity Spectrum Intensity VSI (Von Thun et al., 1988), with a typical DI, the maximum drift ratio $\delta_{r,max}$:

$$\delta_{r,max} = \frac{\delta_{max}}{h} * 100\% \qquad\qquad\qquad (1)$$

where δ_{max} is the maximum displacement at the top of the pier relative to its base and h is the height of the pier.

For VSI = 3 m, the damage can be seen to vary from minor ($\delta_{r,max} < 1\%$) to severe, if not collapse ($\delta_{r,max} > 3\%$). An example of the efficiency of the nonlinear regression equations (Anastasopoulos et al., 2015a) is summarized in Fig. 3b, comparing the observed (FE analysis) to the predicted $\delta_{r,max}$ (multivariate equation). The nonlinear regression equations offer a significant reduction of the deviations between predicted and observed values. Such equations are easily programmable and can be employed for real-time damage assessment.
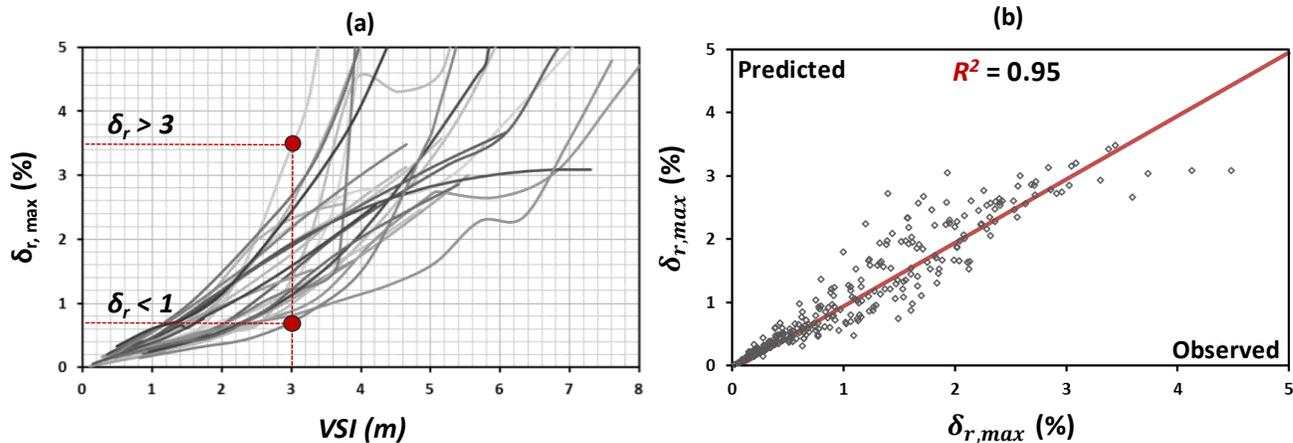

Figure 3. (a) Correlation of $\delta_{r,max}$ as obtained from the FE analysis with VSI; and (b) observed (FE analysis) vs. predicted using the proposed nonlinear regression model equation maximum drift ratio $\delta_{r,max}$.

Simplified Method To Simulate The Seismic Response Of Motorway Bridges

The efficiency of the proposed multivariate equations is highly depended on the accuracy of the FE model used to conduct the dynamic analyses. A SDOF system is a common approximation to analyze the response of a bridge in the transverse direction. In the longitudinal direction, an equivalent SDOF system with rotational fixity at the top (to account for a monolithically connected deck) is commonly assumed. While such simplifications can be reasonable for long multi–span bridges, this is not the case for relatively short motorway overpass bridges, such as the ones examined herein. In such cases, the analysis may entail gross errors if the contribution of the deck, and of the abutment bearings and stoppers is not taken into account.

To quantify the aforementioned gross errors, a typical overpass bridge (A01-TE20) of Attiki Odos Motorway is selected as an illustrative example. As shown in Fig. 4a, the selected system is a symmetric 3-span bridge, representative of about 30% of the bridges of Attiki Odos. A detailed 3D FE model of the bridge–abutment–foundation–soil system was developed in ABAQUS, and used as a benchmark. It is compared both in terms of static pushover and nonlinear dynamic time history analysis with "equivalent" SDOF systems of the bridge, assuming free-end and rotational fixity at the top for the transverse and the longitudinal direction, respectively. As shown in Figs. 4b and 4c, the overly-simplified SDOF models are proven unrealistically conservative, as they ignore the contribution of the lateral and rotational restraint provided by the deck and the system of abutment bearings.

A simplified method was outlined in Anastasopoulos et al. (2015b), considering an equivalent SDOF system of the most vulnerable pier with appropriate springs and dashpots at its top and bottom to account for the contribution of key structural components and nonlinear soil–structure interaction, SSI (Fig. 5). The latter was further extended to account for abutment stoppers, in the longitudinal (Agalianos et al., 2017) and the transverse direction (Sakellariadis et al., 2017), and was further validated for more complex systems.

As schematically illustrated in Fig. 5b, the simplified model is composed of a column having the stiffness, height, and moment–curvature (M–c) response of the pier, and a concentrated mass m_p. The latter refers to the proportion of the deck mass distributed according to the stiffness of the simplified model, relative to that of the entire system. Linear elastic springs

and dashpots are used to model the shear stiffness (K_s) and damping (C_s) of the abutment bearings. In addition, a rotational spring (K_r) and a rotational dashpot (C_r) are added at the top. In the longitudinal direction, this accounts for the flexural stiffness and damping of the deck. In the transverse direction, if the deck was rigidly connected to the abutments, K_r would be equal to the torsional stiffness of the deck. In reality, however, the deck is connected to the abutment through the system of bearings, which has its own rotational stiffness. Hence, the overall rotational stiffness in the transverse direction (K_r) is equal to that of the system of the two rotational springs in parallel.

The stoppers are modelled with special "gap" elements, introduced between the deck and the abutments. The gap elements are activated only in compression, and only after the initial clearance δ_c has been consumed. When the deck collides on the abutment stoppers the behavior of the bridge is different in each direction. In the longitudinal direction the horizontal resistance of the abutment system depends on the retaining wall and the embankment soil. As discussed in Agalianos et al. (2017), the latter is modelled through a nonlinear spring and a linear dashpot (K_{ab}, C_{ab}). In the transverse direction, when the available clearance δ_c is consumed, the deck will collide on the abutment stoppers. In such a case, as discussed in Sakellariadis et al. (2017), it is very important to consider the bending stiffness (K_d) and damping (C_d) of the deck along its strong axis.
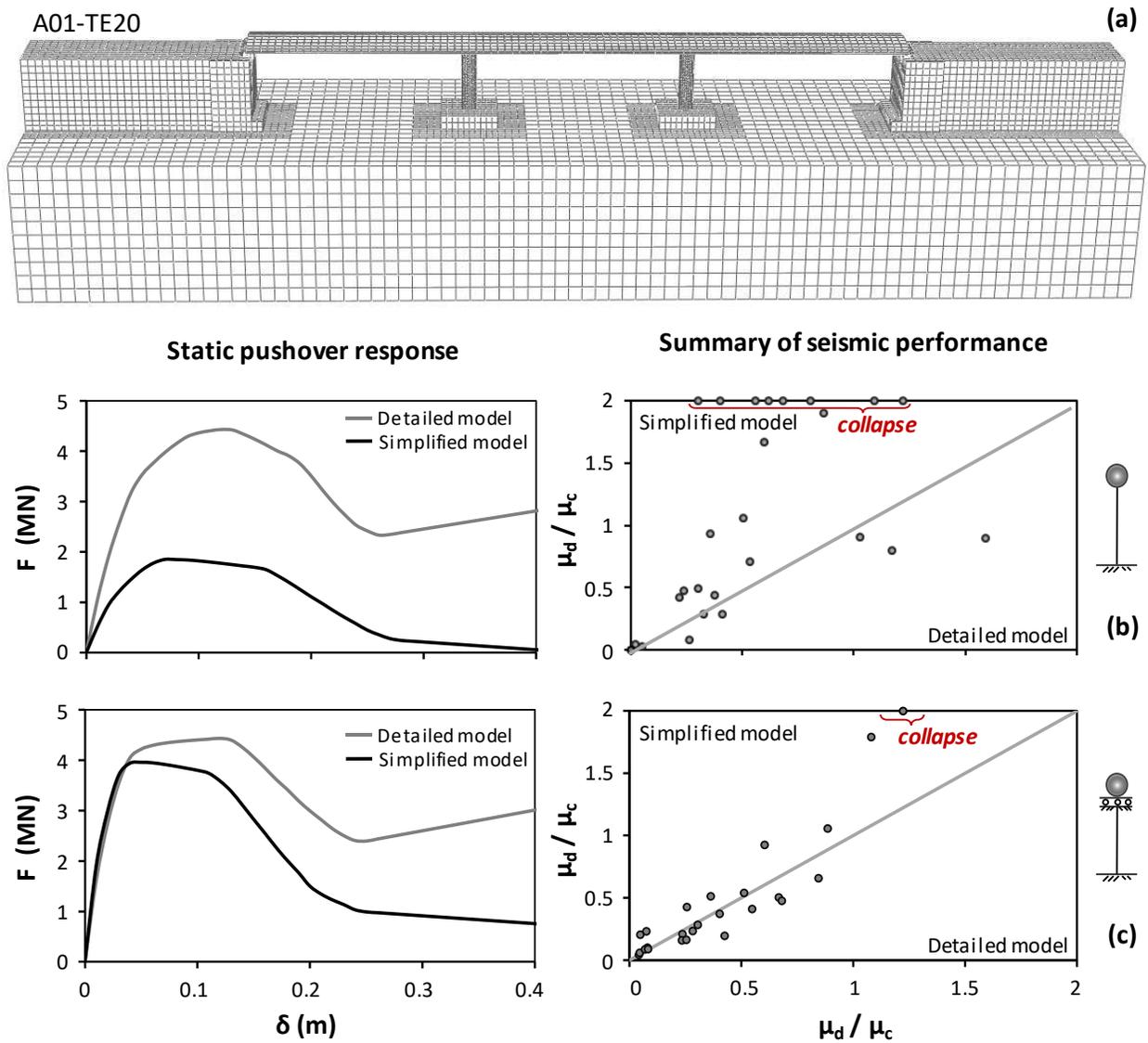

Figure 4. Illustration of the inadequacy of overly-simplified SDOF models: (a) detailed 3D FE model of bridge A01-TE20 used as benchmark; Comparison of SDOF models with the benchmark in static pushover (F–δ) response, and summary of dynamic time history analyses for all seismic excitations–predicted (SDOF models) vs. observed (detailed 3D model) ratio of ductility demand over ductility capacity (μ_d/μ_c): (b) in the transverse; and (c) in the longitudinal direction.

The soil–foundation system is replaced by horizontal, vertical, and rotational springs and dashpots, according to the methodology introduced in Gazetas et al. (2012) and Anastasopoulos & Kontoroupi (2014). The horizontal (K_H and C_H) and vertical (K_V and C_V) springs and dashpots are assumed elastic, and can be directly obtained by published solutions (Gazetas, 1983). For the rotational degree of freedom, a nonlinear rotational spring (K_R) is employed, accompanied by a linear dashpot (C_R).
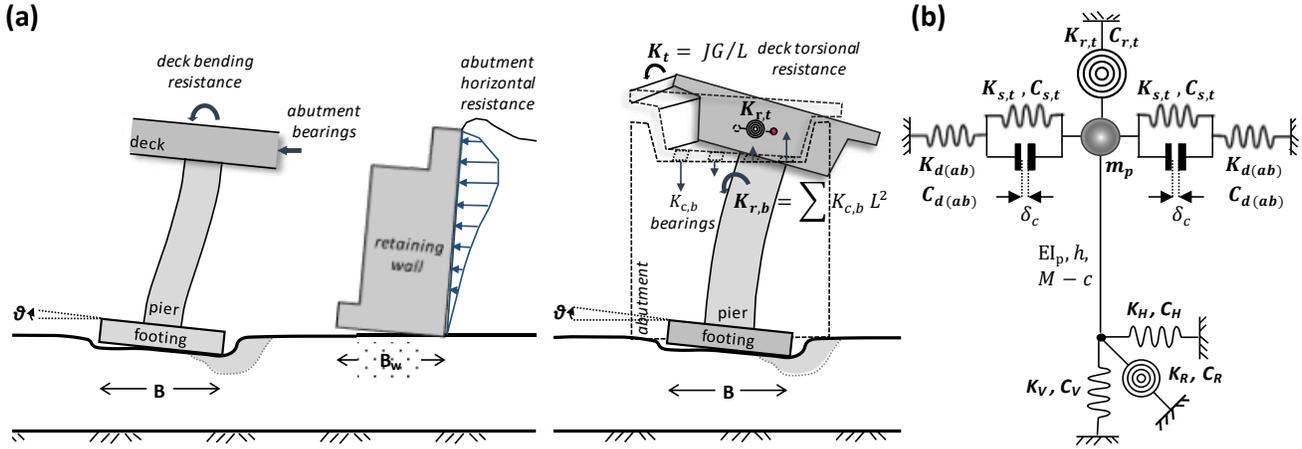

Figure 5. Simplified model accounting for key structural components, nonlinear SSI, and abutment stoppers of clearance δ_c: (a) schematic illustration of key mechanisms; and (b) outline of the model.

The proposed simplified model was validated for 5 bridges of Attiki Odos (Fig. 6). These bridges were carefully selected to cover a wide range of typologies found in the specific motorway, but are also representative of similar motorways around the world. To generalize the conclusions, as much as possible, both the shortest and the longest bridges of Attiki Odos were examined, as well as bridges with single column piers, multi-column piers, and thin-walled piers. A summary of the efficiency of the proposed simplified models is presented in Fig. 7, indicatively for the Lefkada-2003 record in the transverse direction.
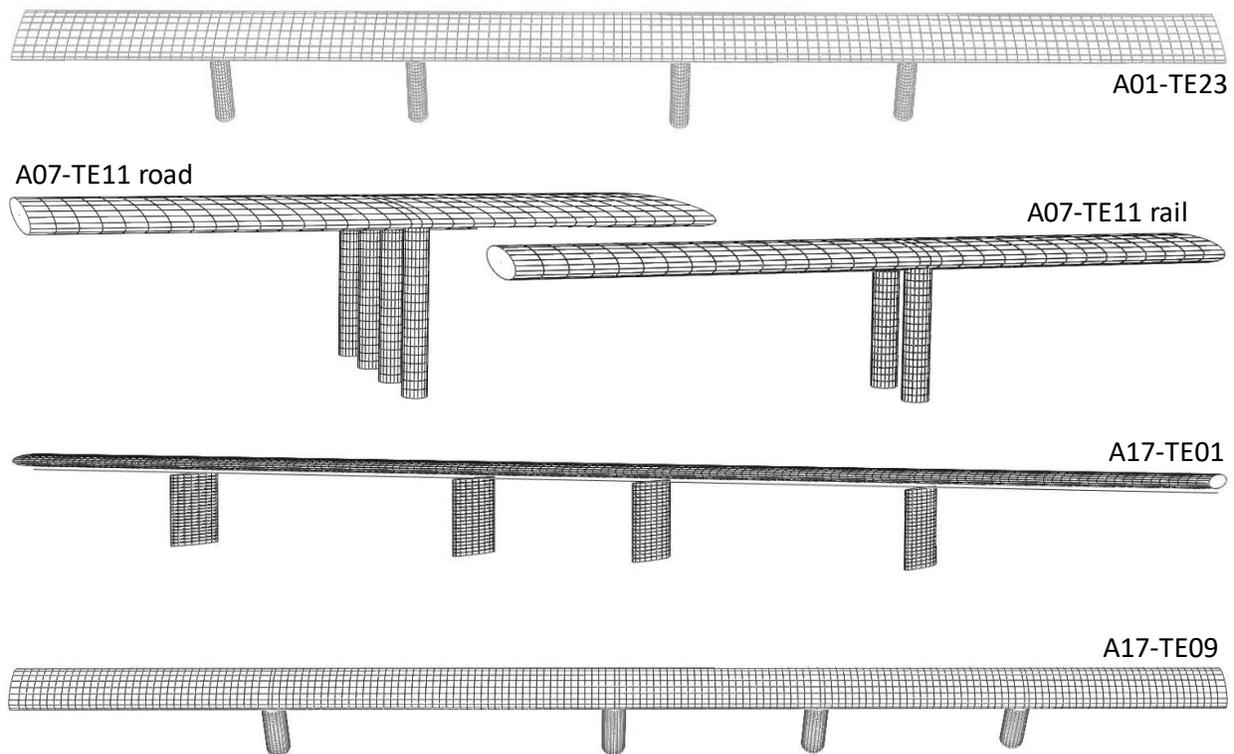

Figure 6. Detailed 3D FE models of 5 bridges of the Attiki Odos motorway, used as benchmarks.

The results indicate that similar bridges may exhibit a substantially different seismic response. For example, road bridge A07-TE11 is almost identical to the rail bridge A07-TE11. Their main difference is that the rail bridge is equipped with abutment stoppers of negligible clearance $\delta_c = 0$, while in the road bridge the deck is only restrained by the bearings at the abutments. This is a small but crucial difference, which makes the rail bridge extremely stiffer, as revealed by its seismic response (Fig. 7). Bridges A17-TE01 and A17-TE09 are also quite similar structural systems. Their main difference lies in the piers, which are thin-walled section piers in the first case. As shown in Fig. 7, such piers are quite stiff in the transverse direction, leading to minimum drift. Most importantly, the results show that the proposed simplified model can accurately capture the response of a variety of motorway bridges, capturing the effect of key structural components, abutment stoppers, and nonlinear SSI.
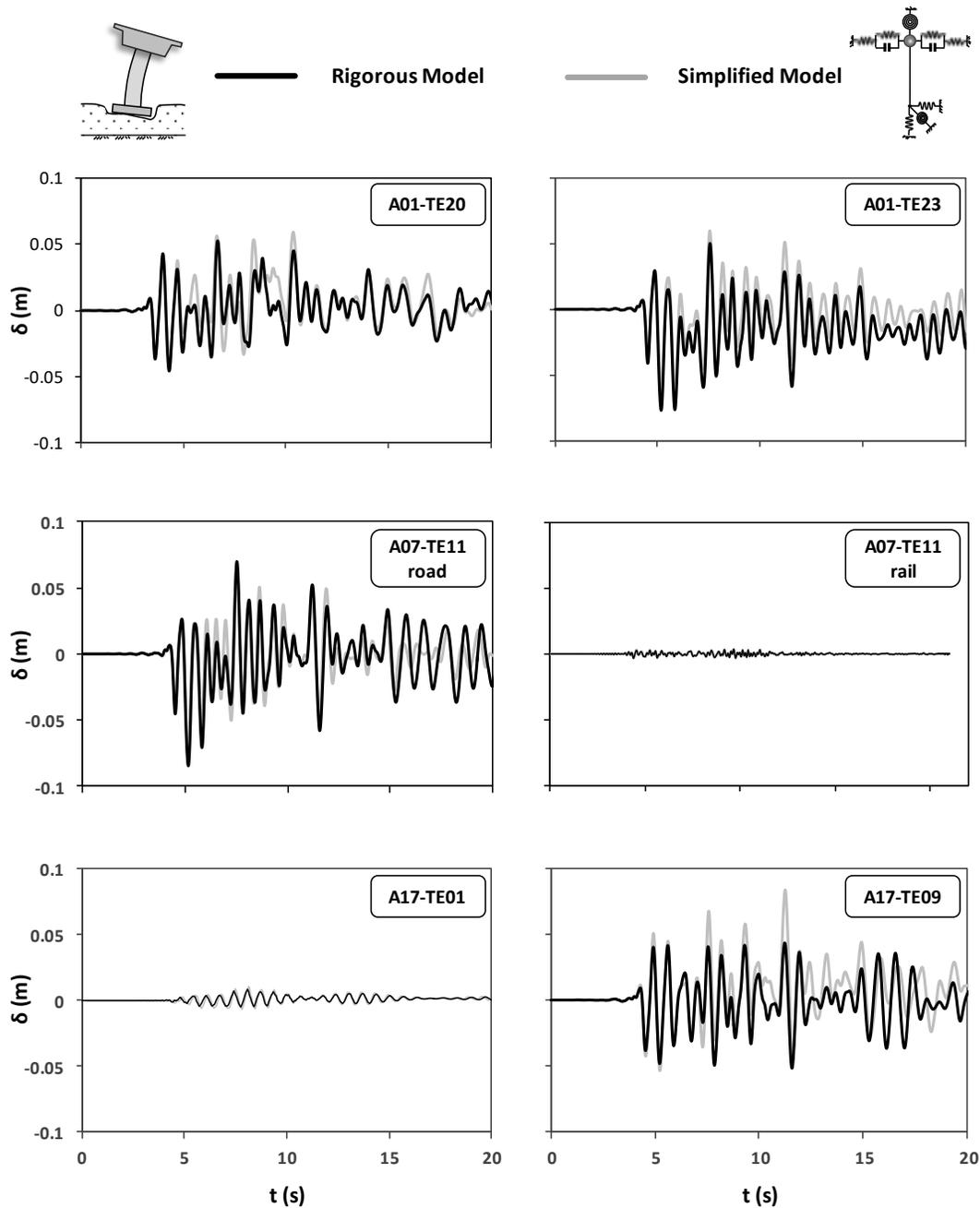

Figure 7. Comparison of the proposed simplified models to the detailed 3D model of the 5 bridges examined: predicted (using the simplified model) vs. observed (using the rigorous 3D model) time histories of deck drift δ , indicatively for the Lefkada-2003 record in the transverse direction.

CLASSIFICATION SCHEME FOR TYPICAL OVERPASS BRIDGES

The developed simplified models account for the contribution of key structural components and SSI, having a major comparative advantage (compared to detailed 3D models) in terms of computational effort. Such models can be used to generate the necessary datasets for the development of the multivariate nonlinear regression model equations for real-time seismic damage assessment. Using such simplified models, it is feasible to apply the proposed methodology to a single bridge and generate the equations for real-time damage assessment. However, a motorway typically includes a few hundreds of bridges. Even using the developed simplified models, analyzing such a number of bridges one-by-one would require a substantial computational effort. Hence, there is a need for classification.

In this context, the classification scheme proposed by Anastasopoulos et al. (2015b) is used herein (Fig. 8). The five examined bridges belong to the same class, which is considered to be the most vulnerable. However, based on the results of Fig. 7, it can be concluded that bridges that belong to the same class can vary significantly in terms of seismic response. Various factors, such as asymmetry, total length, pier typology, and abutment stoppers were proven to significantly affect the seismic performance of the examined bridges calling for a more detailed classification. A well-defined classification criterion is proposed herein, and its validity is assessed for two representative bridges, in each direction of loading.
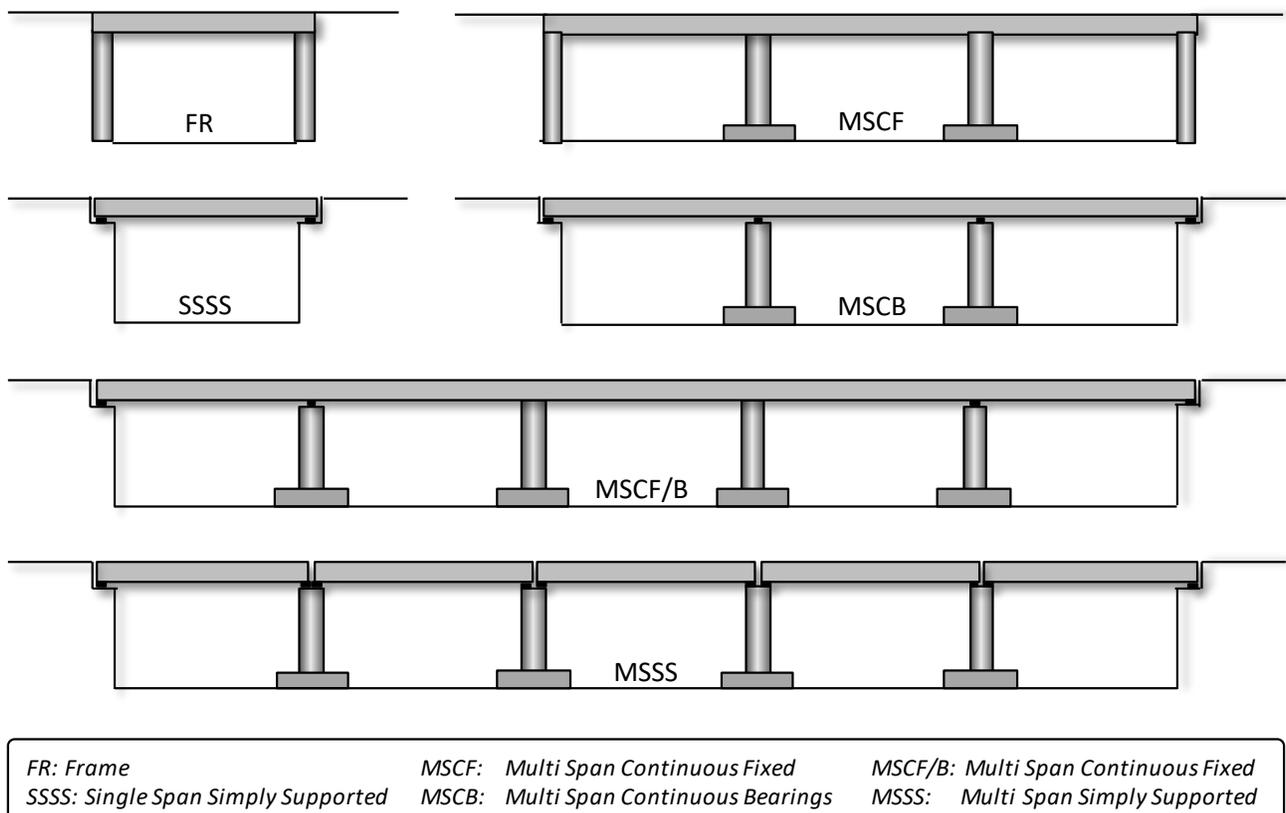

Figure 8. Classification scheme proposed for the bridges of the Attiki Odos motorway (Anastasopoulos et al., 2015b).

Equivalence Criterion For SDOF Systems

A criterion of equivalence for SDOF systems is proposed, based on which two SDOF systems with the same natural period T, yield acceleration a_y, and curvature ductility capacity μ_c, are expected to have similar seismic performance. Two idealized SDOF systems are developed (Fig. 9a), and their seismic response is comparatively assessed using the 30 real records of Fig. 2. A detailed comparison in terms of time histories of drift, δ, is shown in Fig. 9a, referring to one of the strongest records used herein (Takatori_000). A summary comparison for all 30 records in terms of maximum drift δ and ratio of ductility demand over ductility capacity (μ_d/μ_c) is presented in Figs. 9b and 9c, respectively. It may be concluded that the two SDOF systems can be considered equivalent, particularly within the context of a RARE system.
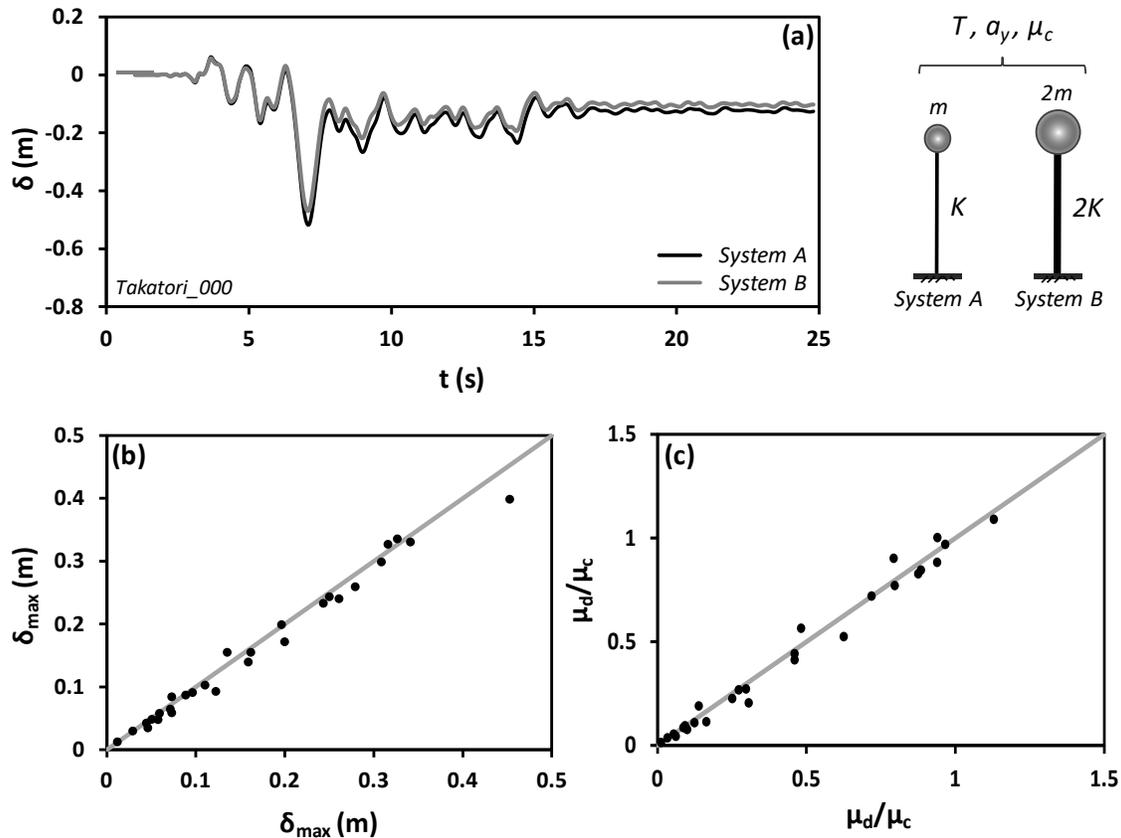
Figure 9. Comparison between two different, but equivalent SDOF systems (A,B), having the same natural period T, design acceleration a_y, and curvature ductility capacity μ_c: (a) detailed comparison of drift δ time histories, indicatively for Takatori_000 record; (b) summary of the 30 dynamic analyses in terms of maximum drift δ_{max} of System A (vertical axis) vs. System B (horizontal axis); and (c) summary comparison in terms of ductility demand over ductility capacity (μ_d/μ_c).

Verification In The Longitudinal Direction

The previous comparison is definitely encouraging, but it only refers to a specific idealized example. To derive a more generalized conclusion, the proposed equivalence criterion is verified for more complex systems. To that end, two bridges of Attiki Odos with similar values of T, a_y and μ_c are selected and examined for each direction of seismic loading. In both cases examined, the comparison is performed using the proposed simplified models. This section deals with the longitudinal direction, and the transverse direction follows.

The selected bridges, A17-TE01 and A18-TE18, are schematically illustrated in Fig. 10. The two bridges are substantially different in terms of total length (156.7 / 112.7 m), deck dimensions (15.1 x 2 / 8.2 x 1.2 m) and piers (1.2 x 9.8 / 0.9 x 4 m). Moreover, while the A17-TE01 bridge has elastomeric bearings in 2 of its 4 piers (M1 and M4), in the case of the A18-TE18 bridge all piers are monolithically connected to the deck. Nevertheless, the relevant simplified models have almost the same natural period (T = 0.37 s and 0.36 s) and yield acceleration (a_y = 0.27g and 0.26g), and fairly similar ductility capacities (μ_c = 19 and 16). Therefore, they meet the criteria of the proposed equivalence criterion. Their performance is assessed on the basis of nonlinear dynamic time history analyses, using a subset of 14 records as seismic excitation, carefully chosen to cover a wide range of excitation characteristics (see Fig. 2).

The performance of the two simplified models is comparatively assessed in Fig. 11. The efficiency of the proposed classification scheme is assessed on the basis of dynamic time history analyses. A detailed comparison of the drift (δ) time histories of the two bridges is presented for two characteristic seismic excitations: Aegion (Fig. 11a) and Kalamata (Fig. 11b). The results of the analyses (for all 14 seismic excitations) are summarized comparing the maximum drift ratio $\delta_{r,max}$ (Fig. 11c) and the ratio of ductility demand over ductility capacity μ_d/μ_c (Fig. 11d) of the two bridges.

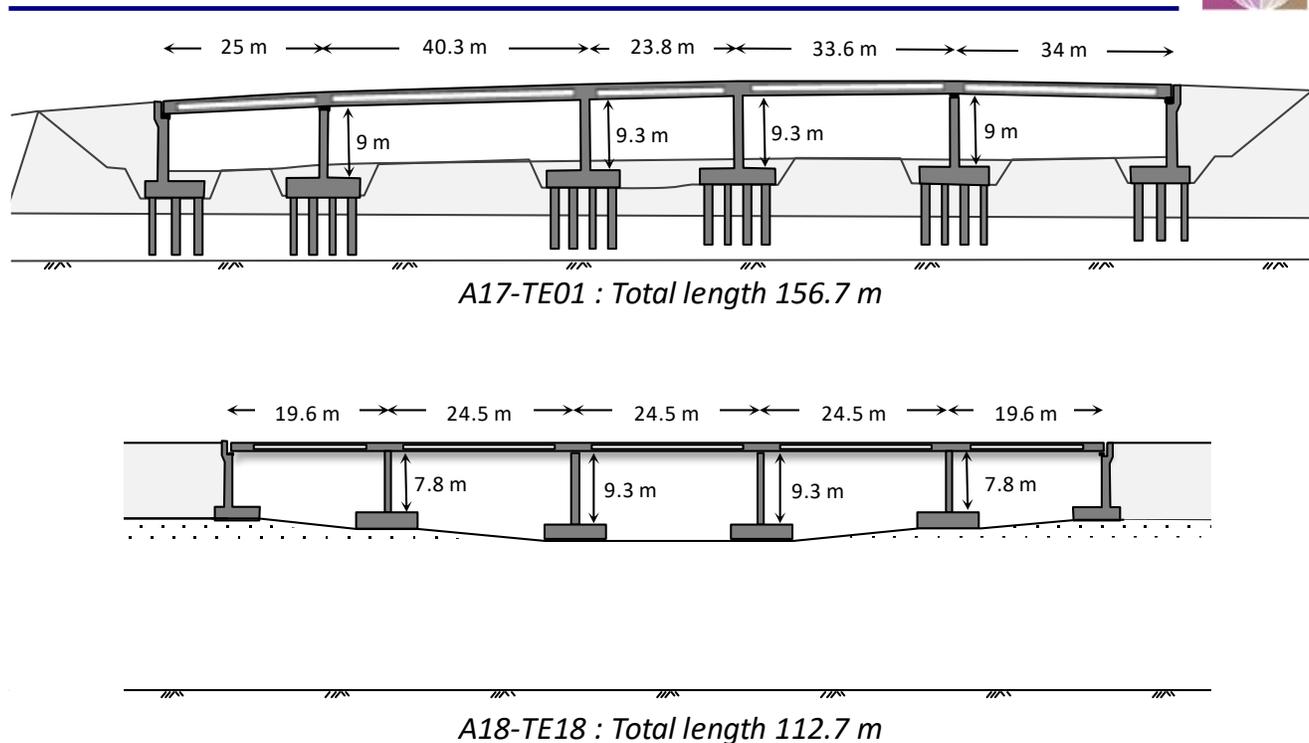A17-TE01 : Total length 156.7 m

A18-TE18 : Total length 112.7 m

Figure 10. Key attributes of the two significantly different bridges of the Attiki Odos motorway used to examine the efficiency of the proposed equivalence criterion in the longitudinal direction.

As shown in Fig. 11, the performance of the two bridges is quite similar, both in terms of $\delta_{r,max}$ and μ_d/μ_c. In addition, the mean average percentage error (MAPE) is estimated:

$$MAPE = \frac{1}{n}\sum_{i=1}^{n}|PE_i| \qquad (2)$$

where: $PE_i = 100\% \left(Y_i - \widehat{Y_i}\right)/ Y_i$ is the percentage error for observation *i* of the actual (observed) damage index value Y_i, and the model-estimated (predicted) damage index value $\widehat{Y_i}$, for observation *i*. The resulting MAPE values give the percentage that the predictors under- or over-estimate the observed values, on average. The mean absolute percentage error (MAPE) is approximately 19% and 26% in terms of $\delta_{r,max}$ and μ_d/μ_c, respectively. In addition, in most cases examined, the drift time histories compare adequately well in terms of frequency content, cycles and maximum values, especially taking into account the significant differences of the two structural systems examined.

The performance of the two bridges is also compared in terms of observed damage states, with reference to Response Limit States (Priestley et al., 1996) for $\delta_{r,max}$ and μ_d/μ_c (Table 1). As shown in Fig. 12a (always referring to the longitudinal direction), in terms of $\delta_{r,max}$ the two bridges are in the same damage state for 12 out of 14 records examined, while 1-state difference is observed for 2 records. In terms of μ_d/μ_c, 11 out of 14 cases are in the same damage state, while 3 out of 14 have 1 state difference (Fig. 12b). In both damage indices there are 0/14 errors (2-state difference). Therefore, the proposed classification scheme can be considered adequate in the context of a RARE system.

Table 1. Performance limit states used to characterise structural damage.

Damage States based on $\delta_{r,max}$		
Minor Damage	Moderate Damage	Severe Damage
< 1%	1–3%	> 3%

Damage States based on μ_d/μ_c			
No essential Damage	Minor Damage	Moderate Damage	Severe Damage
< 20%	20–50 %	50–70 %	> 70 %

Verification In The Transverse Direction

The efficiency of this equivalency criterion is subsequently assessed for more complicated systems in the transverse direction. Two other bridges of Attiki Odos, having similar T, a_y and μ_c are selected for comparison. Bridge A04-TE12 (Fig. 13) is a 3 span, asymmetric bridge with a total length of 44.5 m. The deck is monolithically connected to two multicolumn piers and supported on bearings at the abutments. The developed simplified model has the following characteristics: $T = 1.07$ s, $a_y = 0.098$ g and $\mu_c = 19.9$. The abutment stoppers are also modelled, having a clearance $\delta_c = 140$ mm. The second selected bridge, A05-TE10 (Fig. 13), is substantially different. It is an almost symmetric, much longer (113.3m), 6 span system. The deck is monolithically connected to 5 multicolumn piers and supported on bearings at the abutments. The simplified model has the following characteristics: $T = 1.18$ s, $a_y = 0.074$g and $\mu_c = 22.4$. In this case, the abutment stoppers have a clearance $\delta_c = 150$ mm, which is quite similar to the first bridge. The same subset of seismic records (Fig. 2) is used to compare the seismic performance of the two bridges.
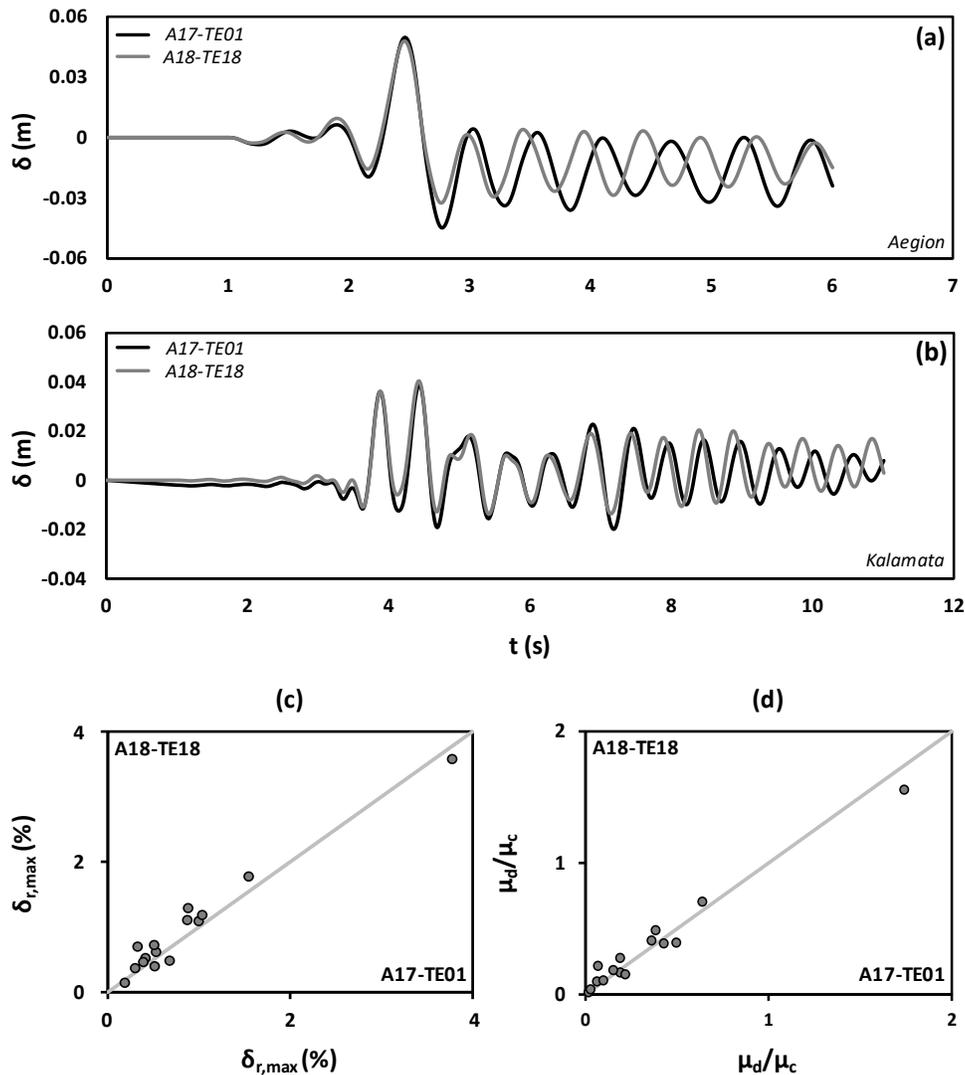

Figure 11. Verification of the equivalence criterion in the longitudinal direction. Comparison of two different bridges of the Attiki Odos motorway (A17-TE01, A18-TE18), which have the same natural period T, design spectral acceleration a_y, and similar curvature ductility capacity μ_c. Detailed comparison in terms of drift δ time histories, indicatively for (a) Aegion; and (b) Kalamata record. Summary of all dynamic analysis results (all 14 records) in terms of: (c) maximum drift ratio $\delta_{r,max}$ of bridge A17-TE01 (vertical axis) vs. that of bridge A18-TE18 (horizontal axis); and (d) ratio of ductility demand over ductility capacity μ_d/μ_c.
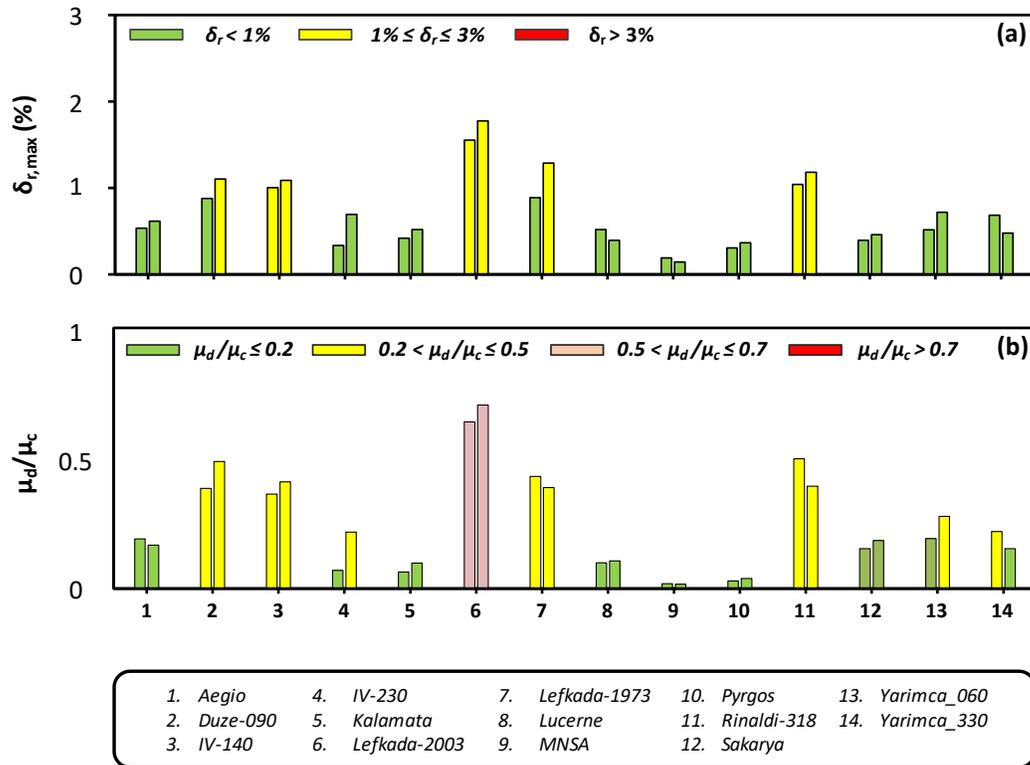
Figure 12. Verification of the equivalence criterion in the longitudinal direction. Comparison of two different bridges of the Attiki Odos motorway (A17-TE01, A18-TE18), which have the same natural period T, design spectral acceleration a_y, and similar curvature ductility capacity μ_c. Comparison in terms of damage states (1st column: A17-TE01; 2nd column: A18-TE18) based on (a) maximum drift ratio $\delta_{r,max}$; and (b) ratio of ductility demand over ductility capacity μ_d/μ_c.

A04-TE12 : Total length 44.5 m
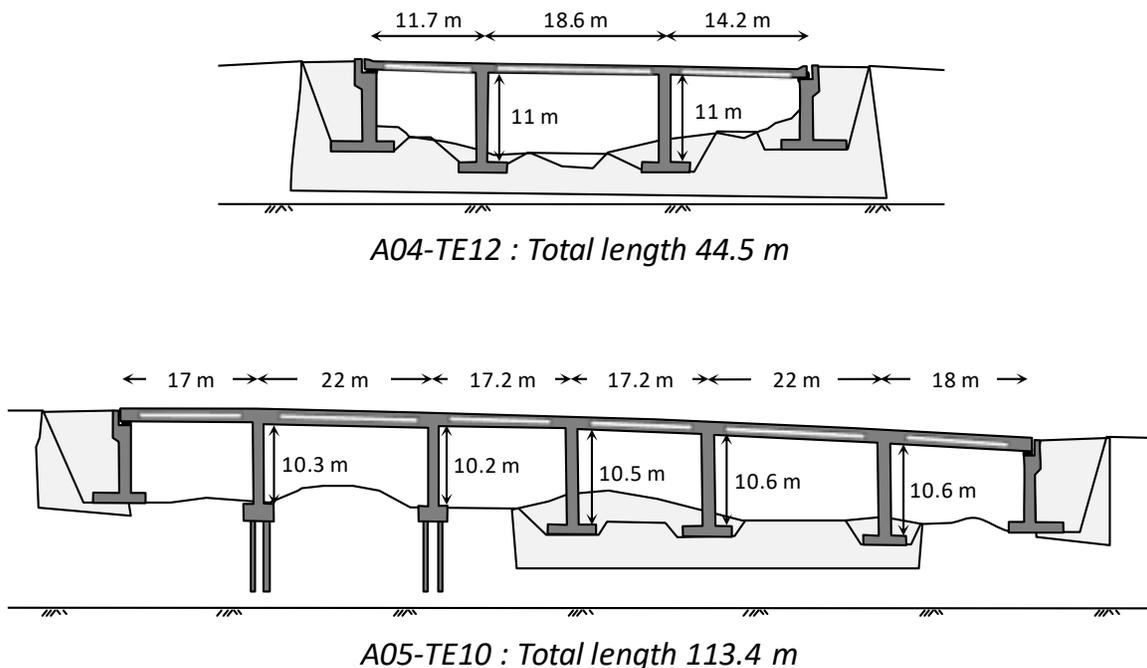

A05-TE10 : Total length 113.4 m

Figure 13. Key attributes of the two significantly different bridges of the Attiki Odos motorway used to examine the efficiency of the proposed classification criterion in the transverse direction.

The seismic performance of the two systems is compared in terms of time histories of deck drift δ. Figures 14a, b present indicatively the results for 2 strong records (Lefkada-2003, and Lucerne). The two bridges are also compared in terms of $\delta_{r,max}$ and μ_d/μ_c in Fig. 14c, d. Despite their differences, the response of the two bridges is quite similar in terms of drift δ time histories. The same applies to the comparison in terms of $\delta_{r,max}$ and μ_d/μ_c, for all 14 seismic records examined. The mean absolute percentage error (MAPE) is approximately 22% and 29% in terms of $\delta_{r,max}$ and μ_d/μ_c, respectively. The observed discrepancies are considered acceptable in the context of a RARE system. As for the longitudinal direction, the comparison is very satisfactory with respect to Damage States. In terms of $\delta_{r,max}$, the two bridges are in the same damage state for 13 out of 14 records (Fig. 15c), while 1-state difference is observed for one record only. In terms of μ_d/μ_c, 10 out of 14 cases are in the same damage state while 4 out of 14 have 1 state difference (Fig. 15d). As previously, in both damage indices there are 0/14 errors (2-state difference).
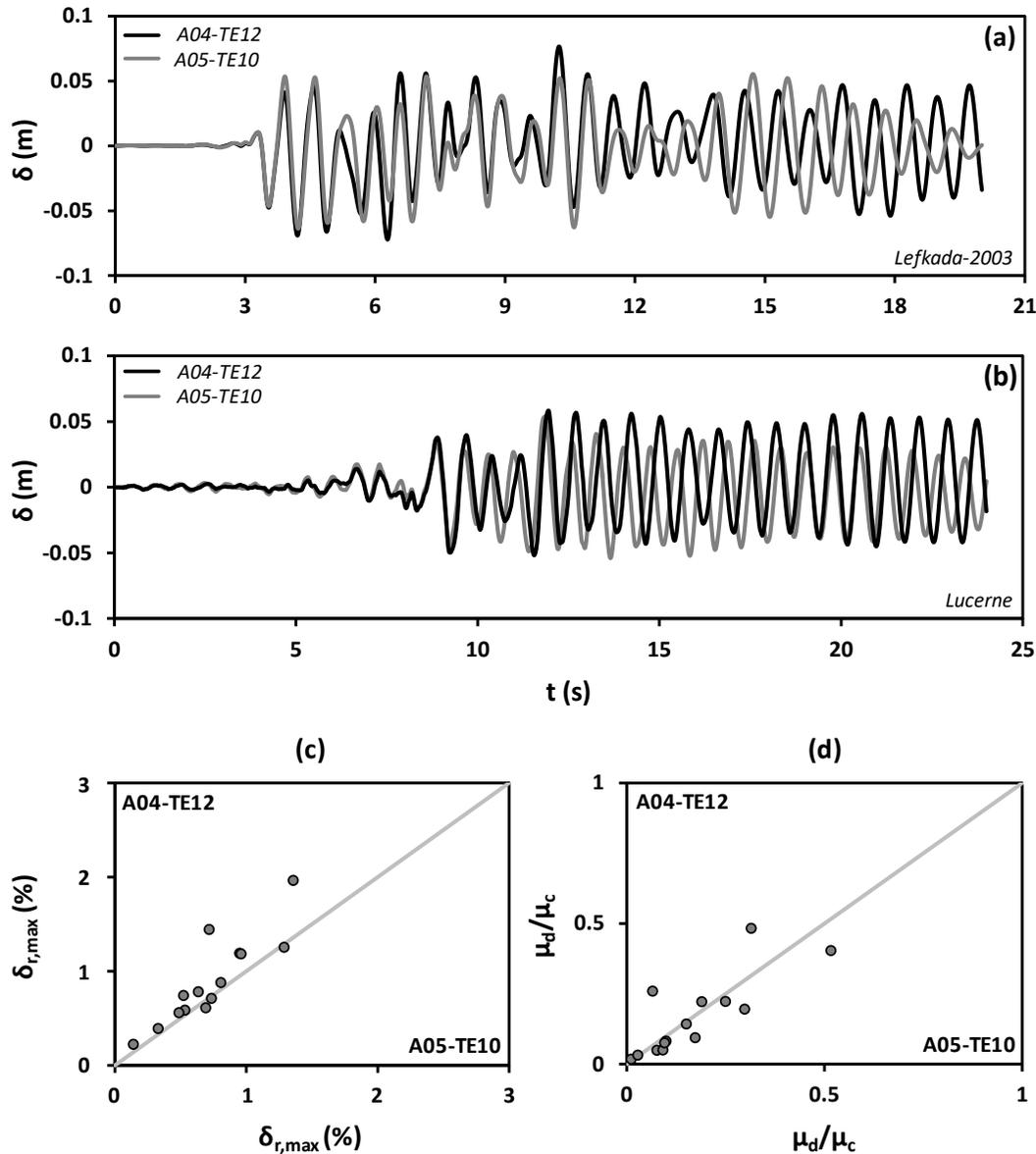

Figure 14. Comparison between the simplified models of two different bridges of the Attiki Odos motorway (A04-TE12, A05-TE10) in the transverse direction with the same natural period (T), design spectral acceleration (a_y) and ductility capacity in terms of drift δ time histories indicatively for (a) Lefkada-2003; and (b) Lucerne records. Summary of the 14 dynamic analyses in terms of observed (FE analysis of A04-TE12) vs. observed (FE analysis of A05-TE10) structural damage expressed with (c) maximum drift ratio ($\delta_{r,max}$); and (d) ratio of ductility demand over ductility capacity (μ_d/μ_c).
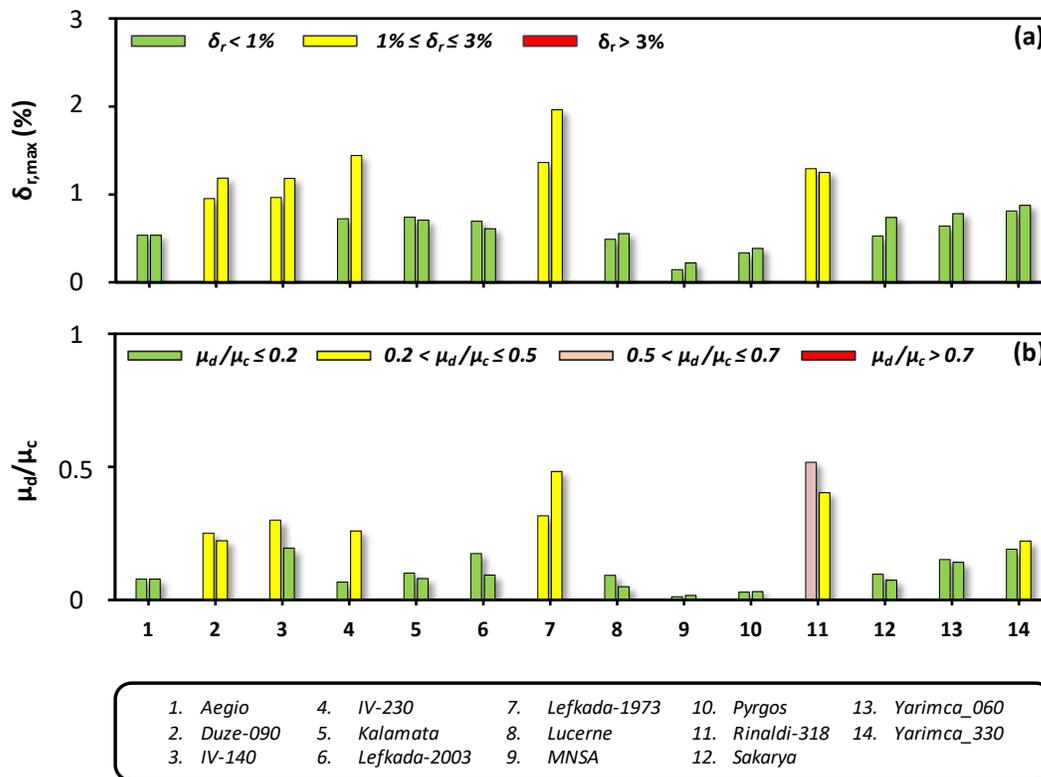
Figure 15. Verification of the equivalence criterion in the longitudinal direction. Comparison of two different bridges of the Attiki Odos motorway (A04-TE12, A05-TE10), which have the same natural period T, design spectral acceleration a_y, and similar curvature ductility capacity μ_c. Comparison in terms of damage states (1st column: A04-TE12; 2nd column: A05-TE10) based on (a) maximum drift ratio $\delta_{r,max}$; and (b) ratio of ductility demand over ductility capacity μ_d/μ_c.

Based on these results, both for transverse and longitudinal direction, the two examined bridges can be considered equivalent in terms of dynamic response, especially for the purposes of a RARE system. Therefore, the efficiency of the examined criterion of equivalence is assessed in more complicated systems and can be considered of more general validity. According to this, two bridges of the same class can be considered equivalent if they have similar: T, a_y, μ_c. Based on this criterion, representative bridges can be selected and used to predict the seismic performance of the corresponding classes.

PILOT APPLICATION TO ATTIKI ODOS MOTORWAY

A pilot application of the RARE methodology is performed on the Attiki Odos motorway, in Athens, Greece. Although the real-time system is not yet functional, a network of accelerograph stations has been installed, and a pilot application of the overall RARE framework is conducted to prove its efficiency in real-life systems.

Accelerograph Network: Design And Installation

A network of 8 accelerographs was installed at "free field" positions along the highway (Fig. 16). The criteria considered in order to define the optimum location for each instrument along the motorway were:

1. Proximity to a highway facility (e.g., toll plaza), in order to facilitate the supply of power.

2. Absence of any major structure in close vicinity, so that the recorded shaking may be characterized "free field" and not influenced by the interaction with nearby structures.

3. Even distribution along the motorway, so that each one records the shaking affecting structures within a radius of 6-8 km around it.

Indeed, in accord with the concept described in the previous sections, the network has been installed so that the recording of each accelerograph may be considered representative of the free field shaking of a different section of the motorway. As such, the free field demand exerted upon each structure is calculated using the readings of the two closest accelerographs.

All readings are tagged both in the time and the space domain within a database maintained in the control unit and administered by the highway network administrator. Hence, they may be manipulated in real time in order to calculate the damage index pertaining to each structure following the methodology presented previously.
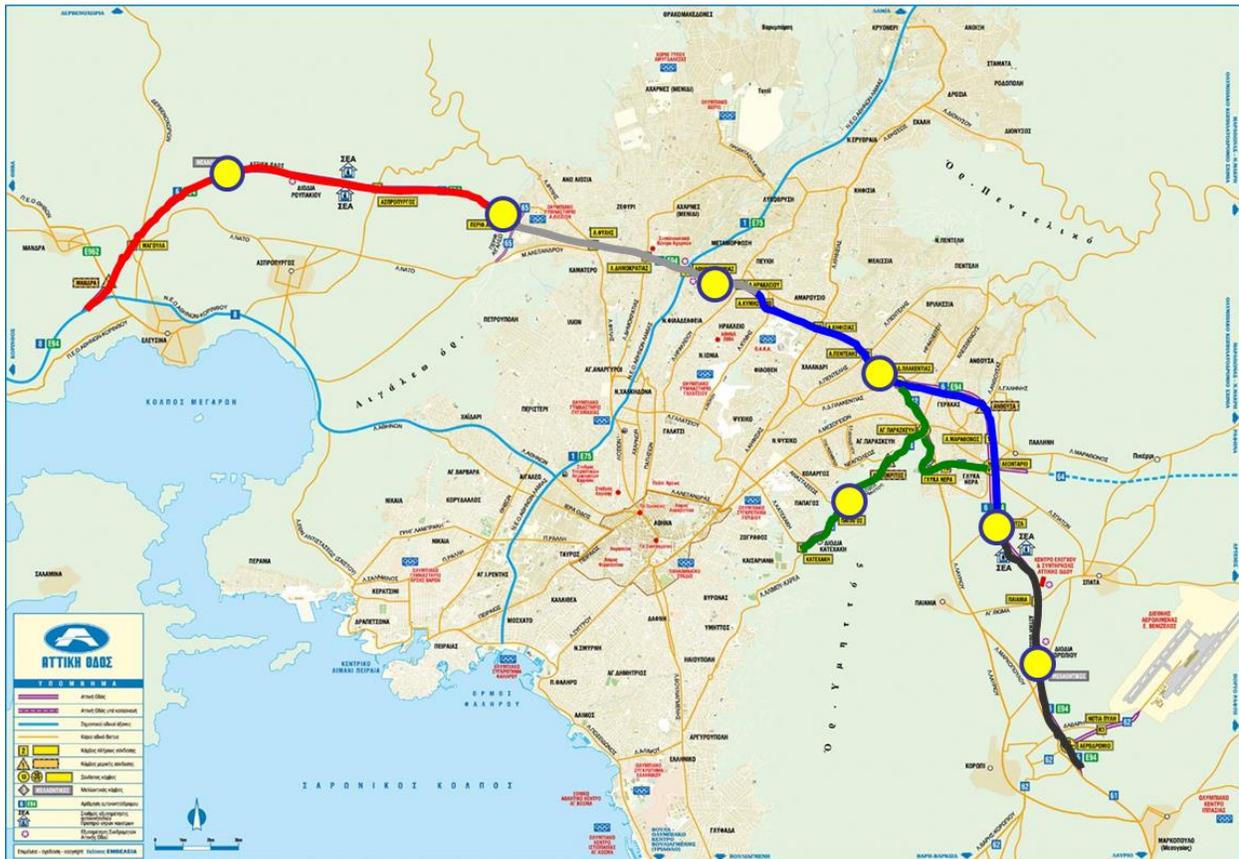

Figure 16. Schematic representation of the installed network.

Accelerograph Network: Implementation

The implemented system, a set of Reftek Strong Motion High Resolution Recorders (with a dynamic range >155dB and a high precision oscillator for precise time-keeping), comprised 8 free-field reference stations automatically broadcasting information when a significant earthquake event occurs (Fig. 17). In order to isolate actual earthquake recordings from traffic induced signals, proper frequency cutoff ranges as well as acceleration threshold amplitudes have been adjusted. The instruments were fixed on purpose-built concrete foundations embedded in the soil. Expanded polystyrene layers were installed between the sides of the concrete foundations and the surrounding soil in order to isolate the recording from the behavior of the surface soil layers around the instrument. For automation purposes, all 8 accelerographs were oriented so that their x recording direction coincides with the global N-S direction, while GPS clocks are by default fixed on each instrument, in order to ensure time and location synchronization. All instruments have been connected with the fiber-optic network running along the highway in order to immediately broadcast recordings and report their own health condition (e.g., faults in power supply or memory) to the control station. Normally, constant external power supply is provided to the instruments from nearby highway facilities; however built-in battery backup is always available to cover any temporary power outage. Similarly, recorded data are constantly transmitted to the control unit servers; yet internal memory cards provide ample backup space able to guarantee an up to 10-days continuous data storage.

Figure 17. View of one accelerograph station. (a) The highway section monitored; (b) The station with the GPS antenna; (c) Close-up of Recording Instruments and wiring.

Development Of Multi–Variate Relations

Using the proposed classification scheme, representative bridges can be selected for the corresponding classes. In the Attiki Odos motorway network, 42/192 of the bridges belong to the MSFC/B class (see Fig. 8). The proposed criterion is applied to these bridges, which are classified in 5 classes for each direction of loading. Thus, 5 characteristic cases can be examined for each direction, leading to a significant reduction of the computational effort. In the present paper, the RARE methodology is applied indicatively for one class using bridge A01-TE20 for both directions. The extended simplified model (Fig. 5) of A01-TE20 bridge is used herein. The latter is shown to be a reasonable approximation for both directions. The computational effort to perform the entire set of analyses using a detailed 3D model (Fig. 4) is prohibitive. The simplified model is used to perform a series of nonlinear dynamic time history analyses using 30 real records as seismic excitation (Fig. 2) scaled to PGA ranging from 0.1 to 1 g. Therefore, a total of 300 analyses are performed, deriving the necessary dataset.

The output of the numerical analyses refers to the structural damage of the bridge, expressed in terms of $\delta_{r,max}$ and μ_d/μ_c, which are two very commonly used DIs, as a function of 19 popular IMs found in the literature. Based on the results of the FE analyses, a dataset correlating the selected DIs with the relevant IMs is developed. The latter is used to develop the nonlinear regression model equations, correlating a single DI with the statistically significant IMs, according to the methodology described in Anastasopoulos et al. (2015a). The resulting linear regression model equations for the 2 selected DIs and for both longitudinal (Eqs. 3, 4) and transverse (Eqs. 5, 6) direction are as follows:

$$\delta_{r,max} = \text{EXP}\left\{\begin{array}{c} 0.32*\text{LN(PGA)}+10.758*\frac{1}{\text{PGV}} - 2.098*\frac{1}{\sqrt{\text{PGD}}} +0.916*\frac{1}{\sqrt{D_{RMS}}} \\ - 0.211*\frac{1}{\sqrt{I_C}} - 9.174*\frac{1}{\sqrt{S_E}} + 167.566*\frac{1}{\text{CAV}} +0.21*\sqrt{\text{VSI}}- \\ - 0.139*\sqrt{I_H} - 0.022*\frac{1}{\text{SMA}} + 3.208*\frac{1}{\text{SMV}} - 0.233*\frac{1}{\text{T}_{mean}} \end{array}\right\} \tag{3}$$

$R^2_{\text{adjusted}} = 0.95$

$$\frac{\mu_d}{\mu_c} = \text{EXP}\left\{\begin{array}{c} 4.233*\sqrt{\text{PGA}} + 7.521*\frac{1}{\text{PGV}} - 2.999*\frac{1}{\text{PGD}} +0.999*\frac{1}{\sqrt{D_{RMS}}} + \\ + 1.91*\sqrt{I_c} - 24.201*\frac{1}{S_E{}^2} + 9992.605*\frac{1}{\text{CAV}^2} - 46.358*\frac{1}{\sqrt{\text{VSI}}} + \\ + 79.057*\frac{1}{I_H} - 0.00032*\frac{1}{\text{SMA}^2} - 2.045*A_{95}{}^2 - 0.727*\frac{1}{\sqrt{T_{mean}}} \end{array}\right\} \tag{4}$$

$R^2_{\text{adjusted}} = 0.95$

$$\delta_{r,max} = \text{EXP}\left[\begin{array}{c} 0.459*\text{LN(PGA)}+ 6.706*\frac{1}{\text{PGV}} -1.681*\frac{1}{\sqrt{\text{PGD}}} - 8.704*A_{RMS}{}^2 +1.12*\frac{1}{\sqrt{D_{RMS}}}- \\ +2.307*\frac{1}{\text{SMV}} + 0.109*\text{LN}(T_P) - 0.22*\frac{1}{\text{T}_{mean}} + 0.071*\sqrt{D_{sig}} \end{array}\right] \tag{5}$$

$R^2_{\text{adjusted}} = 0.96$

$$\frac{\mu_d}{\mu_c} = \text{EXP}\left[\begin{array}{c} 3.955*\sqrt{\text{PGA}} - 2.335*\frac{1}{\text{PGD}} - 27.932*A_{RMS}{}^2 +1.268*\frac{1}{\sqrt{D_{RMS}}} + 5.768*\sqrt{I_c} - \\ -33.871*\frac{1}{\sqrt{\text{VSI}}} + 68.673*\frac{1}{I_H} - - 2.354*A_{95}{}^2 - 1.631*\frac{1}{\sqrt{\text{T}_{mean}}} \end{array}\right] \tag{6}$$

$R^2_{\text{adjusted}} = 0.94$

In Equations 3 through 6, the independent variables (IMs) on the right hand side are all found to be statistically significant, at a 0.95 level of confidence. While including the IMs in the econometric models, attention was given to common model estimation mis-specification issues (multicollinearity, endogeneity, heteroscedasticity, autocorrelation, spurious correlation, etc.). The estimated models are thus well specified. The models' overall statistical fit can be assessed through the Adjusted R-squared, as follows:

$$R^2_{adjusted} = 1 - [(n-1)/(n-p)] * \left[\left(\sum_{i=1}^{n}(Y_i - \hat{Y}_i)^2\right)/(\sum_{i=1}^{n}(Y_i - \bar{Y})^2)\right] \tag{7}$$

where Y_i and $\hat{Y}_i$ are the observed and predicted values, respectively, of the dependent variable (i.e., DI) for observation i ($i = 1, 2, …, n$), $\bar{Y}$ is the observed mean value of the dependent variable, and p is the number of explanatory model parameters. This goodness-of-fit measure gives a relative illustration of the ability of the estimated model to explain the variance in the data, taking into account the number of parameters. This makes the Adjusted R-squared a robust goodness-of-fit measure when comparing competitive models with different number of parameters. Overall the Adjusted R-squared values for the developed nonlinear regression models are quite satisfactory.

Efficiency Of The Simplified Method

The efficiency of the nonlinear regression model equations is examined comparing the predicted structural damage of the simplified model (and therefore of the bridge) by using the corresponding equation, to the observed one, as obtained from the numerical analyses. Figure 18 presents the results of 300 dynamic time history analyses in terms of observed vs. predicted structural damage for the two DIs and for both loading directions. The mean average percentage error (MAPE) is about 16% and 36% for $\delta_{r,max}$ and μ_d/μ_c (both directions), respectively. The MAPE values are considered quite satisfactory. Overall, it can be concluded that the nonlinear regression model equations reduce significantly the discrepancies between predicted and observed values.
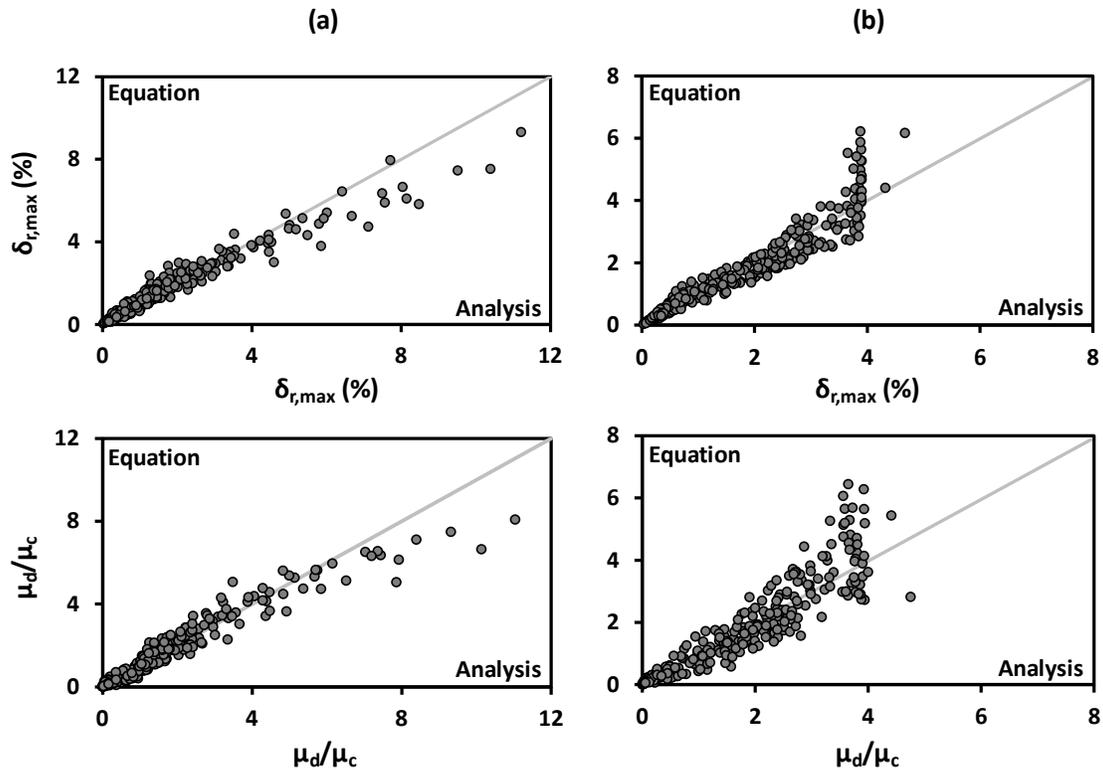
Figure 18. Summary of the 300 dynamic time history analyses in terms of predicted (nonlinear regression model equation) vs. observed (FE analysis using the simplified model) structural damage expressed with the maximum drift ratio ($\delta_{r,max}$) and ductility demand over ductility capacity (μ_d/μ_c) for: (a) the longitudinal; and (b) the transverse direction.

The previously discussed comparison is quite satisfactory, but still, refers to the same dataset that was used to develop the nonlinear regression model equations. It is therefore considered important to verify the predictive capability of the derived equation using out-of-sample data. For this purpose, the 5 out-of-sample historic earthquake records of Fig. 19 are used. A new series of nonlinear dynamic time history analyses are performed, this time using the rigorous 3D model of the A01-TE20 bridge (see Fig 4a). This is a non-trivial test for the nonlinear regression model equations, which were developed using the simplified models, and are now tested against the detailed 3D benchmark model.
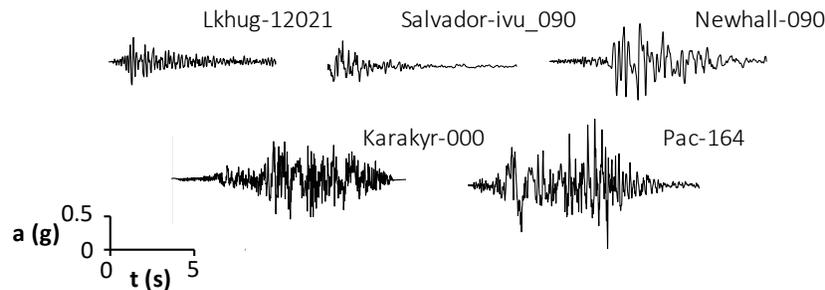

Figure 19. Out-of-sample records used for further verification of the simplified method.

Figure 20 presents a summary of the results of the dynamic time history analyses for the 5 out-of-sample seismic excitations, in terms of predicted (using the nonlinear regression model equations) vs. observed (FE analysis of the detailed 3D model) maximum drift ratio $\delta_{r,max}$ and ductility demand over ductility capacity μ_d/μ_c. The discrepancies are within the expected range and are considered rather minor, given the fact that the equations used for the prediction are based on the simplified model, while the observed structural damage is computed using the rigorous 3D model of the bridge. The results can be seen to test simultaneously the efficiency of the simplified models, and of the nonlinear regression technique.
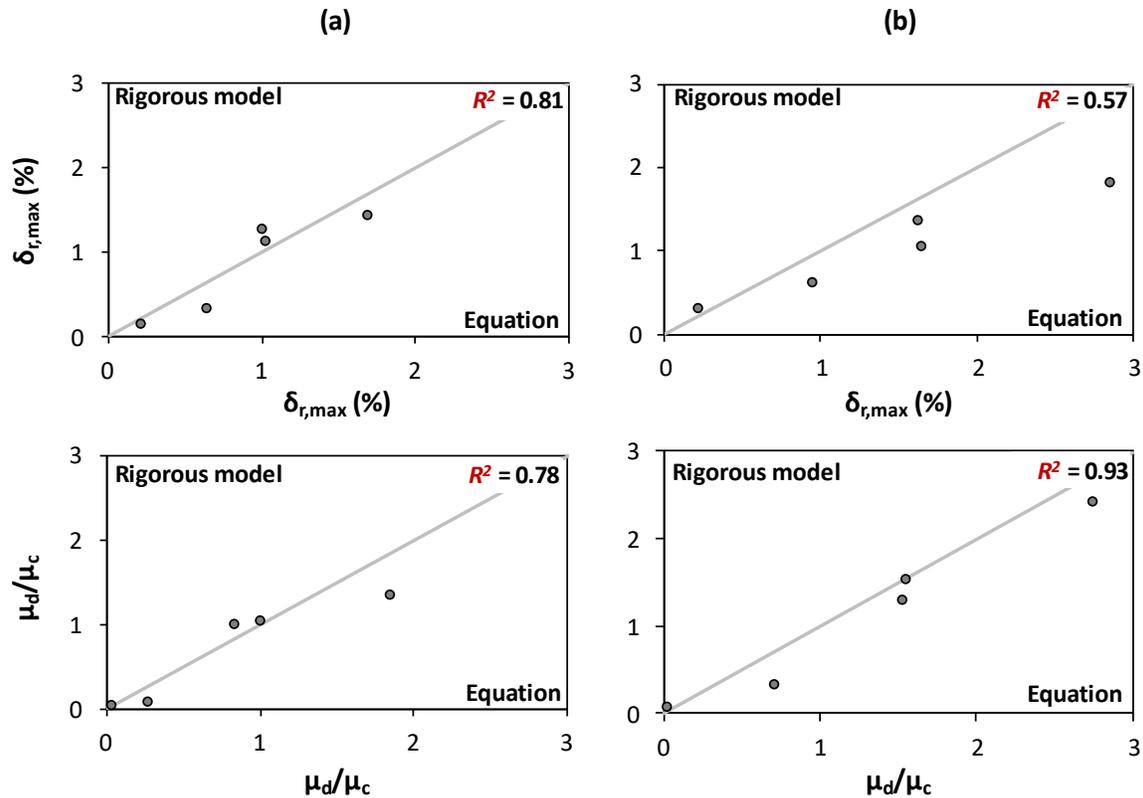
Figure 20. Efficiency of nonlinear regression model equations for out-of-sample historic records. Predicted (nonlinear regression model equation) vs. observed (FE analysis using the detailed 3D model) drift ratio $\delta_{r,max}$ and ductility demand over ductility capacity μ_d/μ_c, for: (a) the longitudinal; and (b) the transverse direction.

Finally, the efficiency of the developed nonlinear regression model equations is comparatively assessed in Fig. 21 in terms of observed damage states, based on the results of the detailed 3D benchmark models, vs. predicted ones, using the developed nonlinear regression model equations. The comparison is performed for the two DIs and for the 5 out-of-sample historic records. The damage states considered are based on typical values of maximum drift ratio $\delta_{r,max}$ and μ_d/μ_c for each damage state, with reference to Response Limit States (Priestley et al., 1996). It is also shown on how many cases (out of the 5 dynamic analyses) the observed damage state is the same with the predicted one and on how many there is no more than one state difference.

In the case of $\delta_{r,max}$, the nonlinear regression model equation correctly predicts the damage state in all cases examined and for both directions. The performance is slightly worse in the case of μ_d/μ_c, in which case the correct prediction rate is 80% (4 out of 5), while a one-state difference is observed in 20% of the examined cases (1 out of 5). Therefore, overall it is shown that the nonlinear regression model equation constitute a satisfactory way to estimate the structural damage of such bridge systems in both directions of seismic loading, as far as a RARE System is concerned.

SYNOPSIS AND CONCLUSIONS

The present paper presents the necessary methodological framework for a rapid response system (RARE) for typical overpass bridges of metropolitan motorway networks. The proposed method is applied in the modern Attiki Odos motorway in Athens, Greece. According to the RARE method, the bridges of a motorway network are classified based on the scheme proposed by Anastasopoulos et al. (2015b), presented in Fig. 8. The MSCF/B class includes about 30% of the bridges of Attiki Odos that is considered the most vulnerable and typical class. The efficiency of the scheme was assessed for 6 bridges (Fig. 6) belonging to this class. For these bridges, simplified models that account for the key structural components and SSI were developed, according to the methodology developed by Anastasopoulos et al. (2015b) (Fig. 5). Their seismic response varies significantly (Fig. 7) calling for further classification.
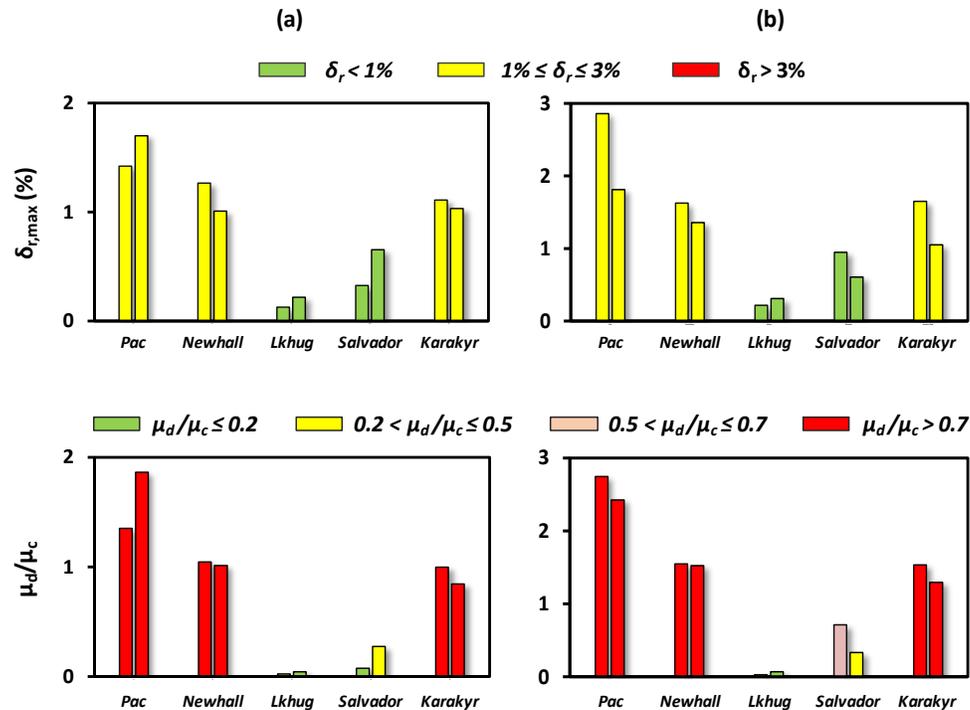
Figure 21. Efficiency of nonlinear regression model equations for out-of-sample historic records. Predicted, using the nonlinear regression model equation (1st column) vs. observed, using the detailed 3D FE model (2nd column) damage state based on maximum drift ratio $\delta_{r,max}$ and ductility demand over ductility capacity μ_d/μ_c, for: (a) the longitudinal; and (b) the transverse direction.

A criterion of equivalence is proposed and validated herein for SDOF systems. According to this, two systems with similar natural period (T), yield acceleration (a_y) and ductility capacity in terms of curvature (μ_c) have similar seismic response (Fig. 9). Its efficiency is further assessed for the proposed simplified models of bridges. To that end, two substantially different bridges are selected in each direction of seismic loading (Figs. 10, 13). Their response is comparatively assessed in terms of nonlinear dynamic time history analysis (Figs. 11, 12, 14 and 15) and shown to be similar. Therefore, it is then applied to the bridges of the Attiki Odos motorway belonging to the MSCF/B class. According to this classification, 5 representative cases can be examined in each direction reducing the computational effort.

The RARE methodology is then applied indicatively for one class using the bridge A01-TE20 as representative in both directions. The extended simplified model (Fig. 5) of the A01-TE20 bridge is developed and its seismic response is examined using 30 historic records (Fig. 2). The records were scaled to PGA from 0.1 to 1 g yielding a dataset of 300 dynamic analyses. Based on the results of the analysis, the dataset was used to develop the nonlinear regression model equations, correlating a single DI ($\delta_{r,max}$, μ_d/μ_c) with the statistically significant IMs. Their efficiency was assessed in terms of predicted (nonlinear regression model equation) vs. observed (FE analysis of rigorous 3D model) structural damage for 5 out of the sample records (Fig. 19) in both directions. The latter is expressed in terms of maximum drift ratio ($\delta_{r,max}$) and ratio of ductility demand over ductility capacity (μ_d/μ_c) (Fig. 20), and in terms of the relevant damage states (Fig. 21). It can be concluded that the multivariate equations (using the simplified model) estimate very satisfactorily the expected structural damage of the bridge, having as a benchmark the rigorous 3D model (Fig. 4a). This methodology can be then applied for each of the 5 proposed classes in each direction. As schematically illustrated in Fig. 1, in the event of an earthquake the real-time system will record seismic accelerations at various locations along the motorway. For each structure, the nearest record(s) will be used to assess the seismic damage employing the multivariate equations for the corresponding class.

ACKNOWLEDGEMENTS

REFERENCES

Agalianos, A., Sakellariadis, L., and Anastasopoulos, I. (2017). "Simplified method for the seismic response of motorway bridges: longitudinal direction – accounting for abutment stoppers." *Bulletin of Earthquake Engineering*.

Anastasopoulos, I. and Kontoroupi, Th. (2014). "Simplified approximate method for analysis of rocking systems accounting for soil inelasticity and foundation uplifting." *Soil Dynamics and Earthquake Engineering*, 56, 28-43.

Anastasopoulos, I., Anastasopoulos, P.Ch., Agalianos, A., and Sakellariadis L. (2015a). "Simple method for real–time seismic damage assessment of bridges." *Soil Dynamics and Earthquake Engineering*, 78, 201-212.

Anastasopoulos, I., Sakellariadis, L., and Agalianos, A. (2015b). "Seismic analysis of motorway bridges accounting for key structural components and nonlinear soil–structure interaction." *Soil Dyn. and Earthquake Engineering*, 78, 127-141.

Arias, A. (1970). "A measure of earthquake intensity." *Hansen RJ (ed) Seismic design for nuclear power plants*, MIT Press, Cambridge, 438-483.

Codermatz, R., Nicolich, R., and Slejko, D. (2003). "Seismic risk assessments and GIS technology: applications to infrastructures in the Friuli-Venezia Giulia region (NE Italy)." *Earthquake Engineering and Structural Dynamics*, 32, 1677-1690.

Dassault Systèmes Simulia Corp. (2013). *ABAQUS 6.13 Standard user's manual*, Providence, RI, USA.

De Groeve, T., Vernaccini, L., and Annunziato, A. (2006). "Global Disaster Alert and Coordination System." *Proc. 3rd International ISCRAM Conference*, Eds. B. Van de Walle and M. Turoff, Newark, 1-10.

Erdik, M., Fahjan, Y., Ozel, O., Alcık, H., Mert, A., and Gul, M. (2003). "Istanbul earthquake rapid response and early warning system." *Bulletin of Earthquake Engineering*, 1(1), 157-63.

Erdik, M., Sesetyan, K., Demircioglu, M.B., Hancilar, U., and Zulfikar, C. (2011). "Rapid earthquake loss assessment after damaging earthquakes." *Soil Dynamics and Earthquake Engineering*, 31, 247-266.

Franchin, P., and Pinto, P.E. (2009). "Allowing Traffic over Mainshock-damaged Bridges." *Journal of Earthquake Engineering*, 13(5), 585-599.

Fountas, G., and Anastasopoulos, P.Ch. (2017). "A random thresholds random parameters ordered probit analysis of highway accident injury-severities." *Analytic Methods in Accident Research*, 15, 1-16.

Fountas, G., Sarwar, T., Anastasopoulos, P.Ch., Blatt, A., and Majka, K. (2017). "Analysis of stationary and dynamic factors affecting highway accident occurrence." *Accident Analysis and Prevention*.

Garini, E., and Gazetas, G. (2013). "Damage potential of near-fault records: sliding displacement against conventional "Intensity Measures." *Bulletin of Earthquake Engineering*, 11, 455-480.

Gazetas, G. (1983). "Analysis of machine foundation vibrations: State of the art." *Soil Dynamics and Earthquake Engineering*, 2, 2-42.

Gazetas, G., Anastasopoulos, I., Adamidis, O., and Kontoroupi, T. (2012), "Nonlinear Rocking Stiffness of Foundations." *Soil Dynamics and Earthquake Engineering*, 47, 83-91.

Housner, G.W. (1952). "Spectrum intensities of strong motion earthquakes." *Proc. of the Symposium on earthquake and blast effects on structures*, EERI, Oakland California, 20–36.

Priestley, M.J.N., Seible, F., and Calvi, G.M. (1996). *Seismic design and retrofit of bridges*, Wiley, New York.

Russo, B., Savolainen, P., Schneider, W., and Anastasopoulos, P.Ch. (2014). "Comparison of factors affecting injury severity in angle collisions by fault status using a random parameters bivariate ordered probit model." *Analytic Methods in Accident Research*, 2, 21-29.

Sakellariadis, L., Agalianos, A., and Anastasopoulos, I. (2017). "Simplified method for the seismic response of motorway bridges: Transverse direction – accounting for abutment stoppers." *Earthquake Engineering & Structural Dynamics*.

Sarwar, T., and Anastasopoulos, P.Ch. (2016a). "A three-stage least squares analysis of post-rehabilitation pavement performance." *Transportation Research Record*, 2589, 97-109.

Sarwar, T., and Anastasopoulos, P.Ch. (2016b). "The effect of long term non-evasive pavement deterioration on accident injury-severity rates: A seemingly unrelated and multivariate equations approach." *Analytic Methods in Accident Research*, 13, 1-15.

Sarwar, T., Fountas, G., and Anastasopoulos, P.Ch. (2017). "Simultaneous estimation of discrete outcome and continuous variable equations: A random effects modeling approach with unrestricted instruments." *Analytic Methods in Accident Research*, 16, 23-34.

Vamvatsikos, D., and Cornell, CA. (2002). "Incremental dynamic analysis Earthquake." *Earthquake Engineering and Structural Dynamics*, 31, 491-514.

Von Thun, J.L., Rochim, L.H., Scott, G.A., and Wilson, J.A. (1988). "Earthquake ground motions for design and analysis of dams." *Earthquake Engineering and Soil Dynamics II—Recent Advances in Ground-Motion Evaluation. Geotechnical Special Publication 20*, ASCE, 463-481.

INTERNATIONAL JOURNAL OF
GEOENGINEERING
CASE HISTORIES

The Journal's Open Access Mission is
generously supported by the following Organizations:

dar
a Sidara company

Geosyntec▷
consultants
engineers | scientists | innovators

CONETEC
MUD BAY DRILLING
LANKELMA
Geotech DRILLING

ENGEO
Expect Excellence